Cancer Cell International

PRIMARY RESEARCH

Open Access

Multi-omics analysis revealed TEK and AXIN2 are potential biomarkers in multifocal papillary thyroid cancer

Ga Hyun Kim[1†], Hye Jin Heo[2†], Ji Wan Kang[1†], Eun-Kyung Kim[2], Seung Eun Baek[2], Keunyoung Kim[3], In Joo Kim[3], Sunghwan Suh[4], Byung-Joo Lee[5], Yun Hak Kim[2,3,6*†] and Kyoungjune Pak[3*†]

Abstract

Background: Papillary thyroid carcinoma (PTC), the most common endocrine cancer, accounts for 80–85% of all malignant thyroid tumors. This study focused on identifying targets that affect the multifocality of PTC. In a previous study, we determined 158 mRNAs related to multifocality in BRAF-mutated PTC using The Cancer Genome Atlas.

Methods: We used multi-omics data (miRNAs and mRNAs) to identify the regulatory mechanisms of the investigated mRNAs. miRNA inhibitors were used to determine the relationship between mRNAs and miRNAs. We analyzed the target protein levels in patient sera using ELISA and immunohistochemical staining of patients' tissues.

Results: We identified 44 miRNAs that showed a negative correlation with mRNA expression. Using in vitro experiments, we identified four miRNAs that inhibit TEK and/or AXIN2 among the target mRNAs. We also showed that the downregulation of *TEK* and *AXIN2* decreased the proliferation and migration of BRAF (+) PTC cells. To evaluate the diagnostic ability of multifocal PTC, we examined serum TEK or AXIN2 in unifocal and multifocal PTC patients using ELISA, and showed that the serum TEK in multifocal PTC patients was higher than that in the unifocal PTC patients. The immunohistochemical study showed higher TEK and AXIN2 expression in multifocal PTC than unifocal PTC.

Conclusions: Both TEK and AXIN2 play a potential role in the multifocality of PTC, and serum TEK may be a diagnostic marker for multifocal PTC.

Keywords: Papillary thyroid carcinoma, BRAF mutation, Multifocality, Multi-omics

Introduction

Thyroid cancer is the most common malignant endocrine tumor and over the last three decades, its incidence has increased continuously worldwide [1, 2]. The most common form of thyroid cancer, papillary thyroid carcinoma (PTC), accounts for 80–85% of all malignant thyroid tumors [3], and has a favorable prognosis with excellent survival rates. However, a minority of patients with PTC develop locoregional recurrence, including cervical lymph node metastases, which eventually leads to mortality in some patients [4]. PTC often presents with multiple anatomically distinct foci within the thyroid, known as multifocal PTC. The reported prevalence of multifocal PTC ranges from 18 to 87% [5, 6]. However, it remains controversial whether multifocal PTCs are (1) multiple synchronous independent primary tumors or

†Ga Hyun Kim, Hye Jin Heo and Ji Wan Kang contributed equally as first authors

†Yun Hak Kim and Kyoungjune Pak contributed equally to this work

*Correspondence: yunhak10510@pusan.ac.kr; ilikechopin@me.com
[2] Department of Anatomy, School of Medicine, Pusan National University, Yangsan, Republic of Korea
[3] Department of Nuclear Medicine and Biomedical Research Institute, Pusan National University Hospital, Busan, Republic of Korea
Full list of author information is available at the end of the article

© The Author(s) 2022. **Open Access** This article is licensed under a Creative Commons Attribution 4.0 International License, which permits use, sharing, adaptation, distribution and reproduction in any medium or format, as long as you give appropriate credit to the original author(s) and the source, provide a link to the Creative Commons licence, and indicate if changes were made. The images or other third party material in this article are included in the article's Creative Commons licence, unless indicated otherwise in a credit line to the material. If material is not included in the article's Creative Commons licence and your intended use is not permitted by statutory regulation or exceeds the permitted use, you will need to obtain permission directly from the copyright holder. To view a copy of this licence, visit http://creativecommons.org/licenses/by/4.0/. The Creative Commons Public Domain Dedication waiver (http://creativecommons.org/publicdomain/zero/1.0/) applies to the data made available in this article, unless otherwise stated in a credit line to the data.

(2) intraglandular dissemination of a single common malignant clone [7, 8]. Previously, we identified the overexpression of 158 mRNAs in multifocal BRAF (+) PTCs, compared to unifocal BRAF (+) PTCs [9]. However, none of the mRNAs in BRAF (+) PTCs showed lower expression than that of the mRNAs in unifocal PTCs [9]. Additionally, none of the mRNAs showed significantly different expression between multifocal and unifocal BRAF (−) PTCs [9]. In addition, mRNAs that were overexpressed in multifocal BRAF (+) PTCs were associated with Wnt- and pluripotency-related pathways, which might account for the difference between multifocal and unifocal BRAF (+) PTCs [9]. The multifocality of PTC has a clinical impact on the treatment of PTC. Although multifocality was not considered as a risk factor in the American Joint Committee on Cancer/Union for International Cancer Control (AJCC/UICC) staging system [4] or American Thyroid Association (ATA) guidelines [4], multifocal PTC has an increased risk of lymph node metastasis, recurrence, and distant metastasis [10, 11]. In addition, multifocality of PTC is associated with the decision making on the optimal extent of surgery for PTCs, if it was identified before the surgery. However, fine needle aspiration cannot be performed for multiple thyroid nodules in clinical settings. The extent of surgical management affects the prognosis of PTC in terms of recurrence [12] and survival [13]. Therefore, adequate information regarding the multifocality of PTC should be provided to improve decision making.

MicroRNAs (miRNAs), a class of non-coding RNAs (15–27 nucleotide RNA molecules), control the expression of mRNA post-transcriptionally by binding to the 3′-untranslated region of mRNA by blocking translation or mRNA degradation [14, 15]. As a large number of miRNAs have been discovered with the continuous progress of technology, the importance of miRNA-mRNA regulatory mechanisms in physiological and pathological states is slowly becoming highlighted [14, 16]. Recently, studies of miRNAs have focused mostly on malignant neoplasms, and miRNAs have been shown to play pivotal roles in various cancers by regulating the expression of their target mRNAs [17–19].

In this study, we hypothesized that miRNAs interact with overexpressed mRNAs in multifocal BRAF (+) PTCs, regulating protein expression. Therefore, we investigated target miRNAs by exploring the following: (1) screening miRNAs that interact with mRNAs in multifocal BRAF (+) PTCs, (2) validation of miRNAs with functional assays, and (3) protein expression in blood samples from patients with PTCs.

Materials and methods

Data acquisition

Clinical characteristics and gene expression data (mRNAs and miRNAs) for PTC were downloaded from the Genomic Data Commons Data Portal (https://gdc-portal.nci.nih.gov/). The Cancer Genome Atlas (TCGA) data were available without restrictions on publications or presentations according to TCGA publication guidelines. Patients were categorized according to BRAF mutation status. In addition, patients were divided into two groups according to the multifocality of PTC. Of the 237 patients with BRAF (+) PTCs, 110 had multifocal PTC and 127 had unifocal PTC according to our previous research [9].

Cell culture

BCPAP (PTC cell line) harboring the BRAF mutation was purchased from DSMZ Korea and was maintained in Roswell Park Memorial Institute (RPMI) 1640 medium containing 10% fetal bovine serum (FBS) and 100 μg/mL penicillin–streptomycin. All cultures were incubated at 37 °C in the presence of 5% CO_2.

microRNA (miRNA) inhibitor transfection

BCPAP cells were transfected with hsa-miR-21a-5p mirVana® miRNA inhibitor (#4,464,084, ID: MH12979, Thermo Fisher Scientific, Waltham, MA, USA), hsa-miR-34a-3p mirVana® miRNA inhibitor (#4,464,084, ID: MH13089, Thermo Fisher Scientific), hsa-miR-203a-3p mirVana® miRNA inhibitor (#4,464,084, ID: MH10152, Thermo Fisher Scientific), hsa-miR-362-3p mirVana® miRNA inhibitor (#4,464,084, ID: MH12485, Thermo Fisher Scientific) and negative control (#4,464,076; Thermo Fisher Scientific). These were used at a final concentration of 30 nM and transfected using Lipofectamine RNAiMAX reagent (Thermo Fisher Scientific).

miRNA assay

For assessment of miRNA expression changes, RT-PCR was performed after miRNA inhibitor transfection. Primers for hsa-miR-21a-5p (#A25576, ID: 477,973 mir), hsa-miR-34a-3p (#A25576, ID: 478,047 mir), hsa-miR-203a-3p (#A25576, ID: 478,316 mir), hsa-miR-362-3p (#A25576, ID: 478,058 mir) was purchased from Thermo Fisher Scientific. miRNA was extracted using miRNeasy Mini Kit (Qiagen, Germany) and reverse transcription was conducted using a TaqMan Advanced miRNA cDNA Synthesis Kit (Thermo Fisher Scientific). Real time-PCR

was performed using the LightCycler TM system (Roche Applied Science, Indianapolis, IN, USA).

siRNA transfection

Negative control (Bioneer, South Korea, #SN-1003) siRNA and target gene siRNA were purchased from Bioneer Corporation (Daejeon, South Korea). Sequences are in Table 1 To create the knockdown cell line, BCPAP cells were seeded at 8×10^4 cells per well in a 6-well plate in RPMI containing 10% FBS. The cells were transfected using DharmaFECT 1 (Thermo Fisher Scientific), as per the manufacturer's instructions, with 300 nM siRNA and incubated for 48 h.

Cell proliferation assay

Cells were seeded at a density of 5×10^3 cells per well in 96-well plates in RPMI containing 10% FBS. After transfection with siRNA for 72 h, BCPAP cell viability was measured using the Cyto X cell viability assay kit from LPS solution Corporation (South Korea). Cyto X (10 µL) was added to each well and incubated for 1 h in a CO_2 incubator. Optical density (OD) values were quantitatively measured at 450 nm using an enzyme-linked immunosorbent assay reader.

Real-time PCR

Total RNA was extracted using the RNeasy mini kit (Qiagen, Germany), miRNA was extracted using miRNeasy mini kit (Qiagen), and cDNA synthesis was performed using a cDNA synthesis kit (Smart gene, South Korea, # SG-CDNAC100). Real-time monitoring of PCR reactions was performed using the LightCycler TM system (Roche Applied Science) and SYBR Green Q-PCR Master Mix with Low Rox (Smart gene, South Korea, #SG-SYBR-ROXL). Glyceraldehyde-3-phosphate dehydrogenase (GAPDH) was used as an internal control and primer sequences for real-time PCR (Table 2).

Wound healing assay

In order to measure the cell migration during wound healing, 48 h after the transfection was carried out (in a 100 mm cell culture dish), BCPAP cells were replated in 24-well plates at a density of 3×10^5 cells per well. Twenty-four hours later, BCPAP cells were cultured in RPMI containing 10% FBS and treated with 1 µg/mL mitomycin-C (Sigma-Aldrich, USA) for 3 h and then wounded with a linear scratch using SPLScar™ Scratcher (SPL Science, South Korea). The average extent of the wound area was evaluated by measuring the width of the wound using ImageJ software.

Three-dimensional (3D) spheroid formation assay

3D spheroid formation was examined by culturing the cells in 200 µL complete medium containing 300 cells in each well and cultured in an ultra-low attachment 96-well plate (Corning, USA, #7007). After 1, 3, and 5 days of incubation, spheroid formation was photographed using phase contrast microscopy (4 × magnification).

Western blot

Cells were washed with PBS, dissolved in radioimmunoprecipitation assay (RIPA) buffer supplemented, and centrifuged at 15,000×*g* for 10 min at 4 °C. Protein concentration was determined by the BCA protein assay (#23,227, Thermo Fisher Scientific) using bovine serum albumin (BSA) as the standard. The proteins were separated by SDS–PAGE and transferred to hybridization nitrocellulose filter membranes (Merck Millipore, USA). The membranes were blocked for non-specific binding with 5% BSA in Tris-buffered saline containing TBS-T (TBS with 0.1% Tween 20) for 1 h at room temperature and then incubated with specific primary antibodies (diluted 1:1000) in TBS-T at 4 °C overnight. After washing with TBS-T three times, the proteins were identified using appropriate secondary antibodies (diluted 1:2000 with 5% BSA). Chemiluminescence was detected with SuperSignal™ West Dura Extended Duration Substrate (Thermo Scientific, USA, #34,075) and visualized using an Amersham Imager 680 (GE Healthcare, USA).

Blood samples

Blood samples were collected from 90 patients with BRAF (+) PTCs (42 unifocal PTCs and 48 multifocal PTCs) who underwent total thyroidectomy at Pusan National University Hospital. Samples were collected within one week of surgery. TEK (Mybiosource, USA, #MBS175906), AXIN2 (Mybiosource, USA, #MBS046455), ADAMTS9

Table 1 Sequence of siRNAs

siRNA	Forward(5′-3′)	Reverse(5′-3′)	Target gene
siTEK	UGAUGAGGUGUAUGAUCUA	UAGAUCAUACACCUCAUCA	TEK
siAXIN2	GACCACAGCCAUUCAGGAA	UUCCUGAAUGGCUGUGGUC	AXIN2
siADAMTS9	CAGGUUACACAACCCAACA	UGUUGGGUUGUGUAACCUG	ADAMTS9
siADAMTSL2	CUCUGUACCCGGAUGACU	UAGUCAUCCGGGUACAGA	ADAMTL2

Table 2 List of RT-PCR primers

Gene	Forward(5′-3′)	Reverse(5′-3′)
ABCB1	CATTCAGGTTTCATTTTGGTG	TCCAACCACGTGTAAATCCTA
ADAMTS9	CATGCAGTTTGTATCCTG	GCGTTCTTTTGAAGTGGACG
ADAMTSL2	ATGTCCACATCTCCAGCA AAC	AGAGTAACCAAGGTGGGCATT
AGPAT5	ACGAGAAAGAGATGCGAA ACA	AAGCAACGTGAGTTGCCTTTA
ARAP3	TGGTTGCCTGTACTATGGTGT	GTGAAATGAGGTCATCACTGG
AXIN2	CTTATCGTGTGGGCAGTA AGA	TCTCTTCATCCTCTCGGATCT
BCAS3	CTGAAGCCAAAGTACAGG ACA	CTCATGCGATTCACTACTCGT
BMPR2	TGAAACAAGTCGAAACTG GAG	ATTAATATTCAGCCGGGTGTC
BOC	TCAGTGTACGTGACCTGG ATT	TTGTAGGAGGTGCCTTTCTCT
B4GALT6	CAGACCAGAGGGAGACTT AGG	CTCTGGCATGAGGTTTACAGA
CCND2	GTGCATTTACACCGACAA CTC	CACACAGAGCAATGAAGGTCT
CD44	CAAATCATTCTGAAGGCT CAA	GGGTGTCCTTATAGGACCAGA
ELOVL2	GCACAAGTATCTTTGGTG GAA	AGGTGGCTCTTGCATATCTTT
ETS1	TGCAGAAAGAGGATGTGA AAC	ATTCTGCAAGGTGTCTGTCTG
FZD3	TTTTTACTATGGCTGGCA GTG	ATCTCAATGCATCAACATCGT
FZD4	AGAGAGTCTGAACTGCAG CAA	GTACTGTGAAGGCAGTGGAGA
HEY2	CGGGATCGGATAAATAAC AGT	TAGGCACTCTCGGAATCCTAT
HIST1H2AC	GTCTGGACGTGGTAAGCA AG	ATGATGCGAGTCTTCTTGTTG
HIST1H4H	GTAAAGGTGGAAAAGGTT TGG	CGTGCTCTGTGTAAGTGACAG
PDGFD	CTAGATTCCCGAACAGCT ACC	TCATCGGACTTGAATGTGATT
PIK3R3	TAAATGACAAATTGCGGG ATA	TGGGATTGTACTGAGCAAGAG
PODXL	CTCAACAGACCTCCAGTC AGA	CACTTTGCCCAGTTACTCTCA
RALB	GAACAGATTCTCCGTGTG AAG	TTCTTGCCATTCTTGTCTTTG
RAPGEF4	CAGCCTTCACAAGGTACA GAA	ATCTTCTCCAACTCTGGCAGT
RNF146	CAAAGAAGGGAGTAGCTG GAC	TCTTCTCCTTCTCCCCTATGA
SLIT3	ACGCCTAGAACAGAACTC CAT	CATACAGGGAGAGCAAGTTGA
TCF4	AGTAAAACAGAAAGGGGC TCA	GCATAGACTGAAGATGGCAAA
TEK	TAAACTTGGACACCATCC AAA	CCAGATCCCTGTGGATAAACT
THSD7B	CCTGCTAAGACCATCACT GAA	TCTCCAAATTATGCTGCTCAC
TRPC4	TTTCCTGTCTTCTCTGTGTGC	CACGGTAATATCATCCACTCG

(Novusbio, USA. #NBP2-66,447) levels in serum were evaluated using an ELISA kit according to the manufacturer's instructions. The results were recorded and analyzed using a microplate reader at 450 nm wavelength (TECAN, Switzerland).

Immunohistochemistry

Human tumor tissue paraffin blocks were processed into sections and deparaffinized, followed by incubation with 3% hydrogen peroxide for 20 min to block the endogenous peroxidases. Next, the tissue sections were blocked with 1% bovine serum albumin for 30 min and then incubated with a polyclonal antibody against AXIN2 and TEK (ABclonal Technology; 1:100 dilution) for overnight at 4 °C. Immunoreaction was visualized using the EnVision detection system kit (Dako), and Mayer's hematoxylin solution was used to stain the nuclei. After staining, images were obtained using an Axio Scan Z1 Digital Slide Scanner (Zeiss, Germany) and analyzed using Zen Blue software (Carl Zeiss. Germany) (magnification: × 100).

Statistical analysis

Statistical differences in clinical variables were analyzed using the chi-square test. To determine the relationship between the 145 mRNAs and total miRNAs, we used the Spearman correlation method based on the Hmisc R package (Hmisc version 4.0–3 and R version 3.4.3). From the correlation analysis results, we selected targets with negative correlations of 0.1 or more, and searched the genes related to the selected miRNAs in Tarbase v.8 (http://carolina.imis.athena-innovation.gr/diana_tools/web/index.php?r=tarbasev8) to confirm the correlation. We sorted the selected miRNAs by 13 pathways identified in previous studies. In vitro experimental data were statistical significance of the differences among groups was determined by a one-way analysis of variance (ANOVA) followed by Tukey's test for multiple comparison using the GraphPad Prism 5 software (GraphPad Software, La Jolla, CA) and differences were considered statistically significant at $p < 0.05$. A comparison of receiver operating characteristic (ROC) was performed to test the difference between the area under the curve of two ROCs from blood samples using MedCalc 19.8 (MedCalc Software Ltd, Ostend, Belgium).

Results

Screening of potential regulatory miRNAs of 145 mRNAs related to multifocality

In the previous study, we reported the enriched genes and pathways in multifocal PTC compared to unifocal PTC [9]. Since multifocal PTC is a more aggressive cancer, we focused on the functional role and regulatory mechanisms of the genes based on their pathways.

To obtain more convincing potential regulatory mechanisms, we used multi-omics data from TCGA. 145 mRNAs in the enriched pathways and whole miRNAs were included in the correlation analysis. miRNAs that correlated negatively with mRNAs were discovered in each pathway as follows [9]: 13 miRNAs in axon guidance, 15 in breast cancer, 29 in ectoderm differentiation, 20 in gastric cancer, 5 in the Hippo signaling pathway, 15 in neural crest differentiation, 31 in O-linked glycosylation, 5 in Phospholipase D signaling pathway, 8 in Rap1 signaling pathway, 16 in Wnt signaling pathway, 11 in signaling pathways regulating pluripotency of stem cells, 16 in TCF dependent signaling in response to Wnt, 12 in the Wnt signaling pathway [20–41] (Fig. 1). To select highly relevant genes, the relationship between mRNAs and miRNAs was confirmed by using Tarbase (Table 3 and Additional file 3: Table S1). Combining the results of Tarbase and correlation analysis, we selected four miRNAs (miR21, miR34a, miR203, and miR362) as potential regulators of target mRNAs.

Selection of target genes through miRNA inhibitors treatment

To validate the relationship between target mRNAs and miRNAs, BCPAP cells were treated with inhibitors of miR21, miR34a, miR203, and miR362. The expression of each miRNA was suppressed after 24 h (Fig. 2A). Four upregulated genes (*TEK*, *AXIN2*, *ADAMTS9*, and *ADAMTSL2*) were shown to be miRNA-regulated genes after treatment with miRNA inhibitors (Fig. 2B). Negative results are presented in Additional file 1: Figure S1.

Functional assays of target mRNAs through siRNA treatment

The knockdown efficiency was assessed by RT-PCR and western blotting, and the results showed that *TEK* and *AXIN2* expression was knocked down effectively by siRNA in BCPAP cells (Fig. 3A, B and C, and Additional file 2). To study whether this downregulation could inhibit the proliferation of BCPAP cells, their proliferation was monitored. As shown in Fig. 3D, the proliferation rate had significantly decreased on day 3 in

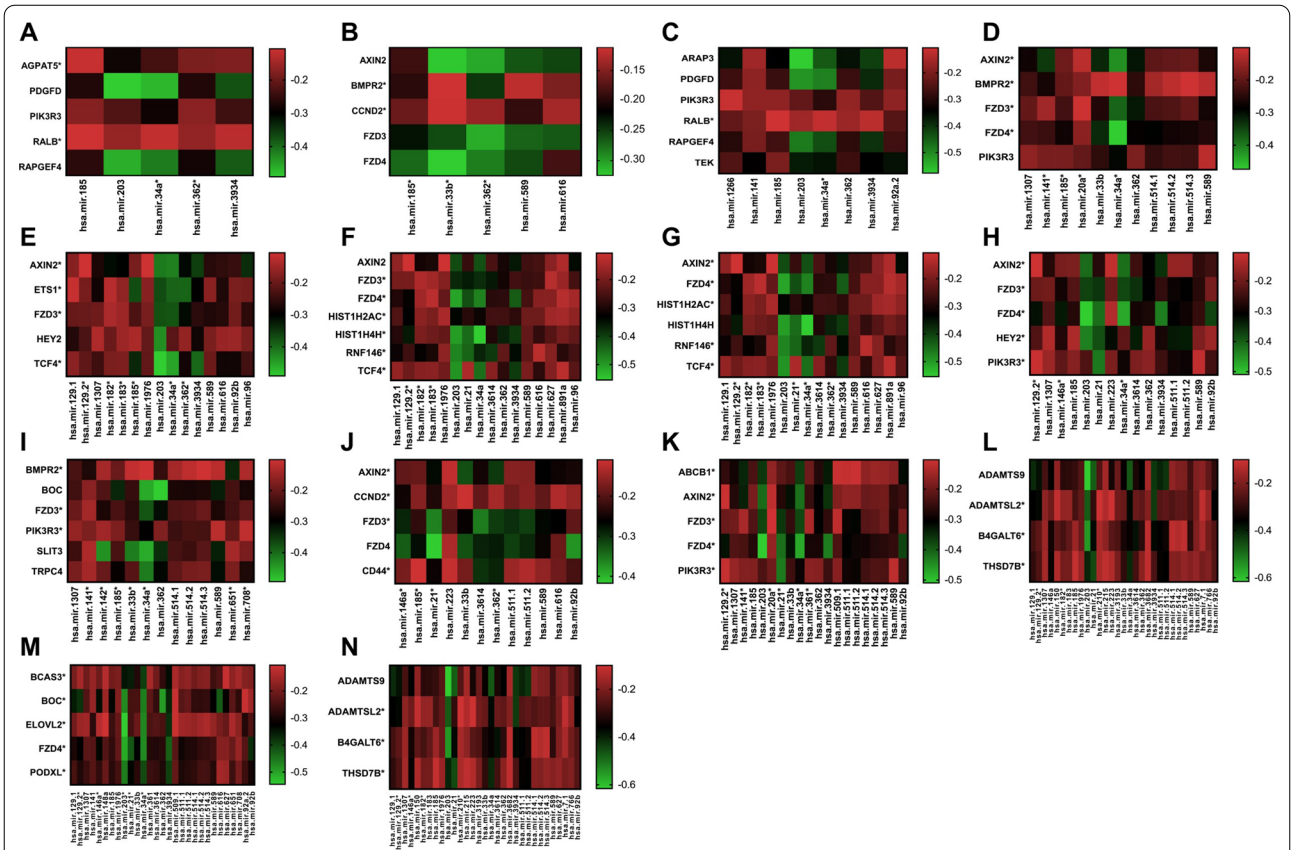

Fig. 1 The correlation between target mRNAs in each pathway and miRNAs in TCGA. **A** Phospholipase D signaling pathways. **B** Hippo signaling pathway. **C** Rap1 signaling pathway. **D** Signaling pathways regulating pluripotency of stem cells. **E** Neural crest differentiation. **F** Signaling by Wnt (**G**) TCF dependent signaling in response to Wnt. **H** Breast cancer. **I** Axon guidance. **J** Wnt signaling pathway and pluripotency. **K** Gastric cancer. **L** Ectoderm differentiation (**M**) O-linked glycosylation. (The * means it is a known target in the Tarbase)

Table 3 The result of correlation analysis. Only values with a correlation coefficient < − 0.1 and P-value < 0.05 were indicated

Gene symbol	miR203 correlation coefficient	miR203 P-value	miR21 correlation coefficient	miR21 P-value	miR34a correlation coefficient	miR34a P-value	miR362 correlation coefficient	miR362 P-value
ABCB1	–	–	–	–	− 0.368	4.61E−09	–	–
ADAMTS9	− 0.616	0	− 0.476	6.66E−15	–	–	–	–
ADAMTSL2	− 0.475	7.77E−15	− 0.295	4.00E−06	–	–	–	–
AXIN2	− 0.414	2.62E−11	− 0.271	2.10E−05	− 0.418	1.60E−11	− 0.306	1.00E−06
B4GALT6	− 0.55	0	–	–	–	–	–	–
BCAS3	− 0.348	3.24E−08	–	–	–	–	–	–
BMPR2	–	–	–	–	–	–	− 0.247	0.000117
BOC	− 0.474	8.44E−15	–	–	–	–	–	–
CCND2	–	–	− 0.241	0.000171	–	–	− 0.139	0.0312
ELOVL2	− 0.545	0	–	–	–	–	–	–
ETS1	− 0.371	3.43E−09	–	–	–	–	–	–
FZD3	–	–	–	–	–	–	− 0.309	1.00E−06
HEY2	− 0.435	1.98E−12	–	–	–	–	–	–
HIST1H2AC	− 0.337	9.20E−08	–	–	–	–	–	–
HIST1H4H	− 0.504	0	–	–	–	–	–	–
PIK3R3	− 0.232	0.000301	–	–	–	–	–	–
PODXL	− 0.461	5.93E−14	–	–	–	–	–	–
RNF146	− 0.476	6.88E−15	–	–	–	–	–	–
TEK	–	–	–	–	− 0.363	7.57E−09	–	–
THSD7B	− 0.406	6.54E−11	− 0.453	1.76E−13	–	–	–	–

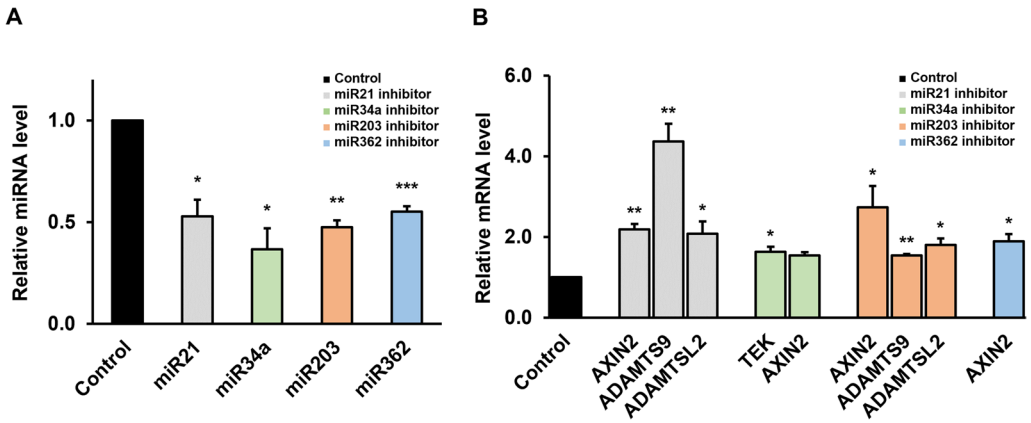

Fig. 2 Inhibition of miR21, miR34a, miR203, and miR362 in BCPAP cells. **A** miRNA inhibitor transfection reduced the expression levels of all four miRNAs by more than 40% in BCPAP as analyzed by qPCR. **B** AXIN2, ADAMTS9 and ADAMTSL2 mRNA expression was up-regulated by miR21 inhibitor (gray), TEK, AXIN2 mRNA expression was up-regulated by miR34a inhibitor (green). And AXIN2, ADAMTS9 and ADAMTSL2 mRNA expression was up-regulated by miR203 inhibitor (orange), AXIN2 mRNA expression was up-regulated by miR362 inhibitor (blue). *$P < 0.05$, **$P < 0.01$, ***$P < 0.001$, compared to the control

siRNA-transfected cells compared to the negative control. In the 3D spheroid formation assay, the BCPAP cells were transfected prior to the generation of spheroids, which were then allowed to grow for 3 days. After 3 days of treatment with *TEK* and *AXIN2* siRNA, the diameter of 3D spheroids was smaller than that of the negative control group, indicating that the *TEK* and *AXIN2* siRNA complexes could significantly inhibit cell growth (Fig. 3E).

To evaluate whether blocking *TEK* and *AXIN2* gene expression affects the oncogenic behavior of BCPAP

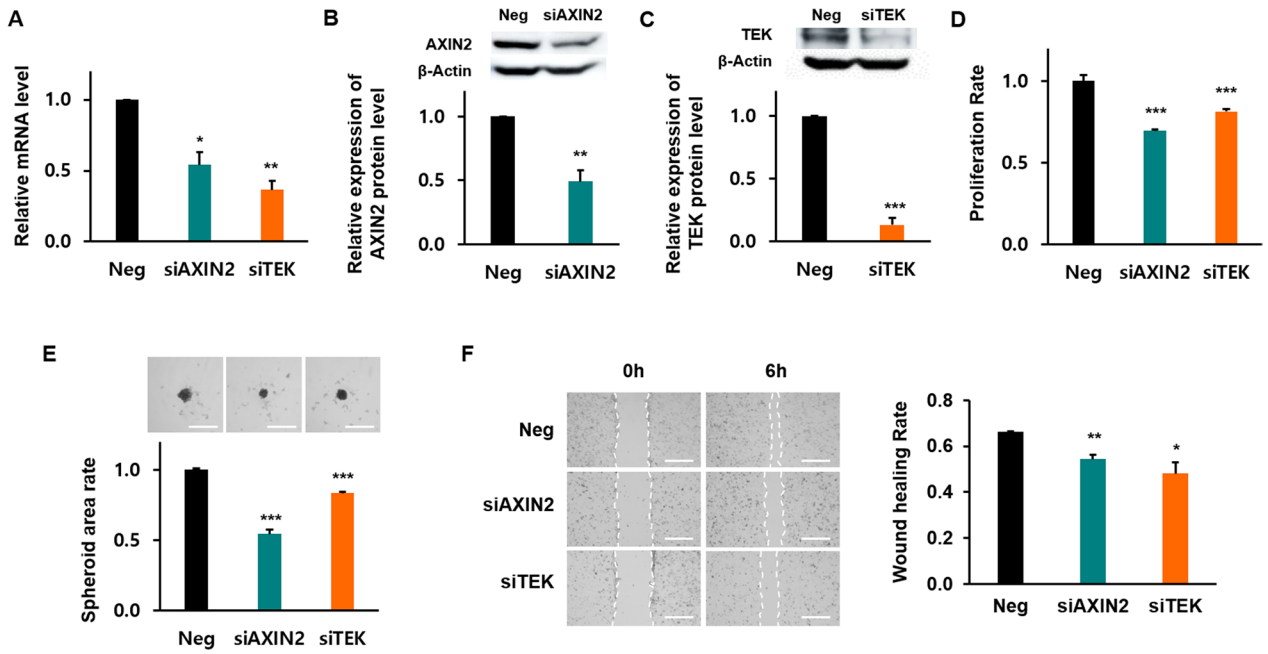

Fig. 3 AXIN2, TEK knockdown inhibits the proliferation, migration of BRAF (+) BCPAP cells. **A** AXIN2, TEK siRNA decreased AXIN2, TEK mRNA expression in BCPAP cells (n = 3). **B**, **C** Western blotting analysis of AXIN2, TEK knockdown efficiency in BCPAP cells. **D** Cell proliferation assay showed that AXIN2, TEK siRNA suppressed the proliferation of BCPAP cells. **E** After transfection with AXIN2, TEK siRNA or control siRNA, spheroid formation was evaluated at 3 days post-seeding. The spheroid area was measured using ImageJ software, encompassing the entire spheroid to the outside edge of spheroid. Scale bar indicates 1000 μm. **F** Wound healing assay showed that AXIN2, TEK knockdown resulted in lower migration capacity in BCPAP cells than in negative control cells. Scale bar indicates 1000 μm. (n = 4) Values are means ± SEM **P* < 0.05, ***P* < 0.01, ****P* < 0.001

cells, we performed a cell migration assay. In a wound-healing assay, the artificial wound gap in plates of the negative siRNA-transfected BCPAP cells was significantly narrower than that of the *TEK*-and *AXIN2* siRNA-transfected BCPAP cells at 6 h (Fig. 3F). *ADAMTS9* and *ADAMTSL2* were excluded from the experiment because of the repeated heterogeneous results.

TEK and AXIN2 from patients with BRAF (+) PTCs: multifocal vs unifocal

42 patients with BRAF (+) unifocal PTCs and 48 patients with BRAF (+) multifocal PTC were included in this analysis. The sizes of the largest tumors were not significantly different (P = 0.5710) between unifocal (1.6 ± 0.7 cm) and multifocal (1.7 ± 0.8 cm) PTCs. The level of TEK in serum from multifocal PTCs was higher than that from unifocal PTCs (P < 0.0001, Fig. 4A), while the level of AXIN2 from multifocal PTCs was lower than that from unifocal PTCs (P < 0.0001, Fig. 4B). To test the performance of TEK and AXIN2, the areas under the curves were compared, which were not significantly different (TEK 0.854; AXIN2 0.779) (Fig. 4C). In the IHC results, the TEK and AXIN2 expression in multifocal PTC are much higher than unifocal PTC (Fig. 4D).

Discussion

The results of the current study are summarized as follows: (1) 13 miRNAs interacted with mRNAs overexpressed in multifocal BRAF (+) PTCs, (2) after validation with miRNA inhibitors, and functional assays, the mRNA expression of *TEK* and *AXIN2* was associated with the multifocality of BRAF (+) PTCs, (3) TEK and AXIN2 in blood samples of patients with multifocal PTCs were significantly different from those with unifocal PTCs.

PTC is the most common form of thyroid cancer with a favorable prognosis; however, a minority of patients develop locoregional recurrence, which eventually leads to mortality in some of these patients [4]. Risk factors that affect the risk of recurrence in PTC include extrathyroidal extension, lymph node involvement, BRAF mutation status, tumor size, and sex [42]. Multifocal PTCs, defined as the presence of two or more than 2 anatomically separated tumor foci in the thyroid gland [43], have been associated with an increased risk of lymph node and distant metastases, as well as disease recurrence [44]. In clinical settings, physicians often encounter patients with multiple thyroid nodules; however, fine needle aspiration of multiple nodules is rarely performed. The selection of thyroid nodules for fine needle aspiration is mainly determined by the cancer probability from ultrasonographic

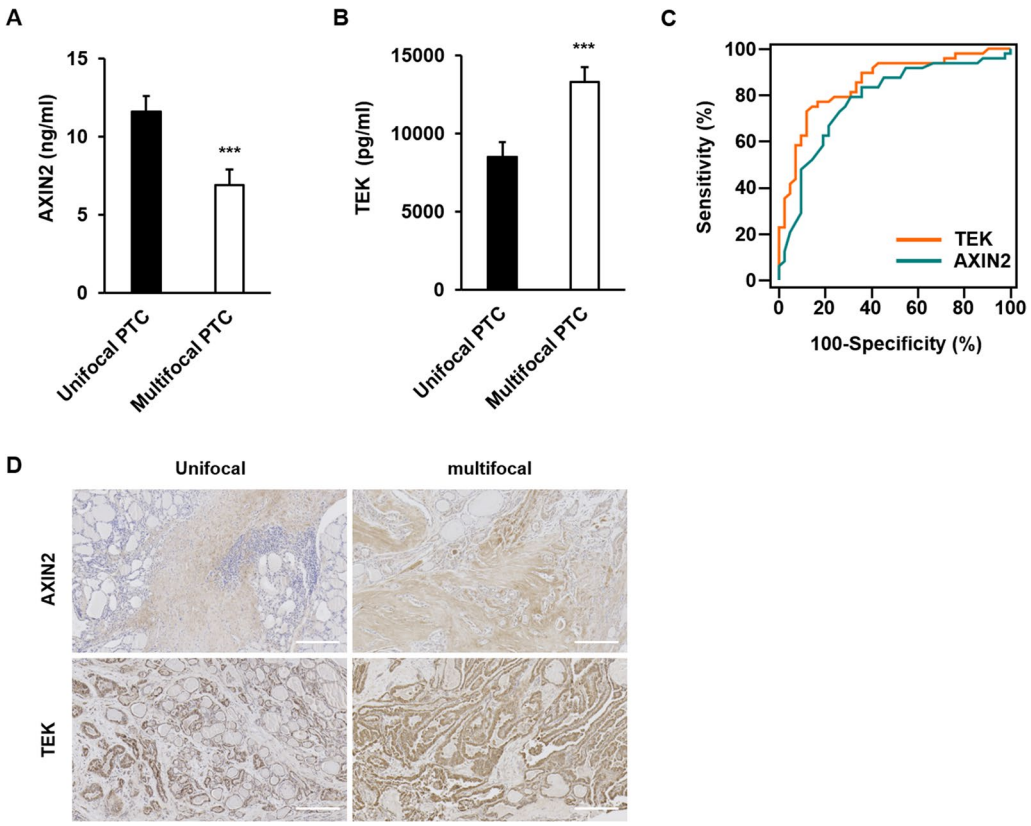

Fig. 4 AXIN2, TEK were assayed using an ELISA and immunohistochemistry (Unifocal PTC, n = 42; Multifocal PTC, n = 48). The AXIN2 (**A**) and TEK (**B**) values in patients' serum (median ± SEM). **C** The receiver operating characteristic (ROC) curve of TEK and AXIN2 in the PTC. **D** AXIN2 and TEK expression levels were confirmed by immunohistochemistry analysis in tumors (scale bar = 200 μm). Values are means ± SEM ***$P < 0.001$

findings, such as the content of the nodule, echogenicity, shape, margin, calcification, and vascularity [45]. According to the ATA guidelines [4], hemithyroidectomy is sufficient for unifocal PTCs without prior irradiation of the head and neck area, a history of familial thyroid cancer, and known lymph node metastasis. In contrast, total thyroidectomy can be recommended if the nodules are confirmed to be malignant in the bilateral lobes [46]. Therefore, decisions regarding the optimal extent of surgery for patients with multiple thyroid nodules should be made after careful consideration.

Based on the results of the correlation analysis of the TCGA data and the in vitro experiments, we identified the oncogenic role of *TEK* and *AXIN2* through miRNA regulatory mechanisms. Although we did not find the exact role of miRNAs in PTC, we observed that 4 miRNAs (miR21, miR34a, miR203, and miR363) inhibition increased the expression of *AXIN2* while *TEK* is only affected by mi34a in BRAF (+) PTC cells. Along with the discovery of the candidate regulatory mechanisms, four miRNAs and two mRNAs were also validated in this study.

TEK (i.e., Tie2) is a receptor tyrosine kinase, which is mainly expressed in endothelial cells and controls vascular regeneration and stabilization [47]. The angiopoietin-Tie system is known to be involved in inflammation, metastasis, and lymphangiogenesis; therefore, multiple clinical trials were performed with selective Tie2 inhibitors [48]. However, the role of TEK in cancer cells remains unclear. Knockdown of TEK increased the proliferation and migration of clear cell renal cell carcinoma [49]; however, the overexpression of TEK in glioma cells was associated with tumor malignancy and drug resistance [50, 51]. Therefore, *TEK* in BRAF (+) PTC cells may affect cell proliferation, invasion, and multifocality.

Since AXIN2 acts as an inhibitor of canonical Wnt signals in normal cells, many studies have focused on elucidating their role as tumor suppressors. However, silencing *AXIN2* decreases the invasive and metastatic characteristics of colon cancer [52]. In the current study, *AXIN2* expression was higher in multifocal PTC than in unifocal PTC, and knockdown of *AXIN2* inhibited cell proliferation in BRAF (+) PTC cells. In addition, it was found that the expression of *Wnt* target

genes, including AXIN2, differed based on the presence/absence of the BRAF mutation [53]. Our previous results showed that *AXIN2* expression did not differ between BRAF (−) multifocal and unifocal PTC [9]. Taken together, these results suggest that the role of *AXIN2* may be different for each cancer, and BRAF mutations may affect *AXIN2* expression.

In this study, the level of TEK in the serum from multifocal PTC patients was higher than that in unifocal PTCs, while the level of AXIN2 from multifocal PTCs was lower than that from unifocal PTCs. On the contrary, a lower level of AXIN2 was observed in multifocal PTC. The biological reason for this phenomenon may be the half-life of the protein [54, 55] as well as post-transcriptional and post-translational modifications. According to a recent analysis, protein expression correlates with the corresponding mRNA level by 20–40%, and mRNA expression levels are not completely representative of the corresponding protein concentration [56, 57]. Therefore, serum TEK and AXIN2 levels may provide information on multifocality in patients with BRAF (+) PTC in a separate way.

Summarily, we used big database to obtain potential regulatory mechanism of target genes and highlighted the interaction of miRNAs with the expression of target genes and proteins in multifocal BRAF (+) PTC. miRNA inhibition increased the mRNA expression of *TEK* and *AXIN2*. Serum TEK and AXIN2 levels may provide information on the multifocality of BRAF (+) PTC. Although there are some limitations, this study provides evidences for the regulatory mechanism of the genes and their contribution to PTC multifocality for the first time.

Supplementary Information

The online version contains supplementary material available at https://doi.org/10.1186/s12935-022-02606-x.

Additional file 1: Figure S1. Expression changes of mRNAs in BRAF (+) BCPAP cells after treatment with miR21 (gray), miR34a (green), miR203 (orange), and miR362 (blue) inhibitors at 24hr.

Additional file 2: Figure S2. Raw Western blot data.

Additional file 3: Table S1. The results of Tarbase.

Acknowledgements
Not applicable.

Author contributions
GH, HJ, JW, YH, and KJ wrote the article. GH, HJ, EK, and SE performed experimental evaluation. JW, KY, and IJ analyzed omics data. SH and BJ designed figures. YH, and KJ supervised the article. All authors read and approved the final manuscript.

Funding
This work was supported by the National Research Foundation of Korea (2020R1C1C1003741, 2018R1A5A2023879 and 2020R1A2C109956511).

Availability of data and materials
The datasets used or analysed during the current study are available from the corresponding author on reasonable request.

Declarations

Ethics approval and consent to participate
The biospecimens and data used for this study were provided by the Biobank of Pusan National University Hospital, a member of the Korea Biobank Network. Informed consent for the collection, storage, and use of blood samples was obtained from each patient. This study was approved by the Institutional Review Board of Pusan National University Hospital (PNUH-2005-013-091).

Consent for publication
Not applicable.

Competing interests
The authors declare that they have no competing interests.

Author details
[1]Interdisciplinary Program of Genomic Data Science, Pusan National University, Yangsan, Republic of Korea. [2]Department of Anatomy, School of Medicine, Pusan National University, Yangsan, Republic of Korea. [3]Department of Nuclear Medicine and Biomedical Research Institute, Pusan National University Hospital, Busan, Republic of Korea. [4]Department of Internal Medicine, Dong-A University College of Medicine, Busan, Republic of Korea. [5]Department of Otorhinolaryngology-Head and Neck Surgery, Pusan National University Hospital, Busan, Republic of Korea. [6]Department of Biomedical Informatics, School of Medicine, Pusan National University, Yangsan, Republic of Korea.

Received: 16 October 2021 Accepted: 2 May 2022
Published online: 12 May 2022

References

1. Lee JH, Lee ES, Kim YS. Clinicopathologic significance of BRAF V600E mutation in papillary carcinomas of the thyroid: a meta-analysis. Cancer. 2007;110(1):38–46.
2. Ciampi R, Mian C, Fugazzola L, Cosci B, Romei C, Barollo S, et al. Evidence of a low prevalence of RAS mutations in a large medullary thyroid cancer series. Thyroid. 2013;23(1):50–7.
3. Cabanillas ME, McFadden DG, Durante C. Thyroid cancer. Lancet. 2016;388(10061):2783–95.
4. Haugen BR, Alexander EK, Bible KC, Doherty GM, Mandel SJ, Nikiforov YE, et al. 2015 American thyroid association management guidelines for adult patients with thyroid nodules and differentiated thyroid cancer: The American thyroid association guidelines task force on thyroid nodules and differentiated thyroid cancer. Thyroid. 2016;26(1):1–133.
5. Wang W, Su X, He K, Wang Y, Wang H, Wang H, et al. Comparison of the clinicopathologic features and prognosis of bilateral versus unilateral multifocal papillary thyroid cancer: an updated study with more than 2000 consecutive patients. Cancer. 2016;122(2):198–206.
6. Iacobone M, Jansson S, Barczynski M, Goretzki P. Multifocal papillary thyroid carcinoma–a consensus report of the European Society of Endocrine Surgeons (ESES). Langenbecks Arch Surg. 2014;399(2):141–54.
7. Iida F, Yonekura M, Miyakawa M. Study of intraglandular dissemination of thyroid cancer. Cancer. 1969;24(4):764–71.
8. Russell WO, Ibanez ML, Clark RL, White EC. Thyroid carcinoma. Classification, intraglandular dissemination, and clinicopathological study based upon whole organ sections of 80 glands. Cancer. 1963;16:1425–60.
9. Pak K, Suh S, Goh TS, Kim SJ, Oh SO, Seok JW, et al. BRAF-positive multifocal and unifocal papillary thyroid cancer show different messenger RNA expressions. Clin Endocrinol. 2019;90(4):601–7.
10. Shattuck TM, Westra WH, Ladenson PW, Arnold A. Independent clonal origins of distinct tumor foci in multifocal papillary thyroid carcinoma. N Engl J Med. 2005;352(23):2406–12.

11. Kim HJ, Sohn SY, Jang HW, Kim SW, Chung JH. Multifocality, but not bilaterality, is a predictor of disease recurrence/persistence of papillary thyroid carcinoma. World J Surg. 2013;37(2):376–84.
12. Grant CS, Hay ID, Gough IR, Bergstralh EJ, Goellner JR, McConahey WM. Local recurrence in papillary thyroid carcinoma: is extent of surgical resection important? Surgery. 1988;104(6):954–62.
13. Bilimoria KY, Bentrem DJ, Ko CY, Stewart AK, Winchester DP, Talamonti MS, et al. Extent of surgery affects survival for papillary thyroid cancer. Ann Surg. 2007;246(3):375–81 (**discussion 81 4**).
14. Cai Y, Yu X, Hu S, Yu J. A brief review on the mechanisms of miRNA regulation. Genom Proteom Bioinform. 2009;7(4):147–54.
15. Kim K, Ko Y, Oh H, Ha M, Kang J, Kwon EJ, et al. MicroRNA-98 is a prognostic factor for asbestos-induced mesothelioma. J Toxicol Environ Health A. 2020;83(3):126–34.
16. Drakaki A, Iliopoulos D. MicroRNA gene networks in oncogenesis. Curr Genom. 2009;10(1):35–41.
17. Choudhury Y, Tay FC, Lam DH, Sandanaraj E, Tang C, Ang BT, et al. Attenuated adenosine-to-inosine editing of microRNA-376a* promotes invasiveness of glioblastoma cells. J Clin Invest. 2012;122(11):4059–76.
18. Hayes J, Peruzzi PP, Lawler S. MicroRNAs in cancer: biomarkers, functions and therapy. Trends Mol Med. 2014;20(8):460–9.
19. Stahlhut C, Slack FJ. MicroRNAs and the cancer phenotype: profiling, signatures and clinical implications. Genome Med. 2013;5(12):111.
20. Balakrishnan I, Yang X, Brown J, Ramakrishnan A, Torok-Storb B, Kabos P, et al. Genome-wide analysis of miRNA-mRNA interactions in marrow stromal cells. Stem Cells. 2014;32(3):662–73.
21. Boudreau RL, Jiang P, Gilmore BL, Spengler RM, Tirabassi R, Nelson JA, et al. Transcriptome-wide discovery of microRNA binding sites in human brain. Neuron. 2014;81(2):294–305.
22. Brock M, Trenkmann M, Gay RE, Michel BA, Gay S, Fischler M, et al. Interleukin-6 modulates the expression of the bone morphogenic protein receptor type II through a novel STAT3-microRNA cluster 17/92 pathway. Circ Res. 2009;104(10):1184–91.
23. Cantini L, Isella C, Petti C, Picco G, Chiola S, Ficarra E, et al. MicroRNA-mRNA interactions underlying colorectal cancer molecular subtypes. Nat Commun. 2015;6:8878.
24. Cao J, Shen Y, Zhu L, Xu Y, Zhou Y, Wu Z, et al. miR-129-3p controls cilia assembly by regulating CP110 and actin dynamics. Nat Cell Biol. 2012;14(7):697–706.
25. Chang TC, Wentzel EA, Kent OA, Ramachandran K, Mullendore M, Lee KH, et al. Transactivation of miR-34a by p53 broadly influences gene expression and promotes apoptosis. Mol Cell. 2007;26(5):745–52.
26. Gabriely G, Wurdinger T, Kesari S, Esau CC, Burchard J, Linsley PS, et al. MicroRNA 21 promotes glioma invasion by targeting matrix metalloproteinase regulators. Mol Cell Biol. 2008;28(17):5369–80.
27. Gottwein E, Corcoran DL, Mukherjee N, Skalsky RL, Hafner M, Nusbaum JD, et al. Viral microRNA targetome of KSHV-infected primary effusion lymphoma cell lines. Cell Host Microbe. 2011;10(5):515–26.
28. Haecker I, Gay LA, Yang Y, Hu J, Morse AM, McIntyre LM, et al. Ago HITS-CLIP expands understanding of Kaposi's sarcoma-associated herpesvirus miRNA function in primary effusion lymphomas. PLoS Pathog. 2012;8(8):e1002884.
29. Kaller M, Liffers ST, Oeljeklaus S, Kuhlmann K, Roh S, Hoffmann R, et al. Genome-wide characterization of miR-34a induced changes in protein and mRNA expression by a combined pulsed SILAC and microarray analysis. Mol Cell Proteom. 2011;10(8):M111010462.
30. Kameswaran V, Bramswig NC, McKenna LB, Penn M, Schug J, Hand NJ, et al. Epigenetic regulation of the DLK1-MEG3 microRNA cluster in human type 2 diabetic islets. Cell Metab. 2014;19(1):135–45.
31. Karginov FV, Hannon GJ. Remodeling of Ago2-mRNA interactions upon cellular stress reflects miRNA complementarity and correlates with altered translation rates. Genes Dev. 2013;27(14):1624–32.
32. Kiga K, Mimuro H, Suzuki M, Shinozaki-Ushiku A, Kobayashi T, Sanada T, et al. Epigenetic silencing of miR-210 increases the proliferation of gastric epithelium during chronic Helicobacter pylori infection. Nat Commun. 2014;5:4497.
33. Kishore S, Jaskiewicz L, Burger L, Hausser J, Khorshid M, Zavolan M. A quantitative analysis of CLIP methods for identifying binding sites of RNA-binding proteins. Nat Methods. 2011;8(7):559–64.
34. Krishnan K, Steptoe AL, Martin HC, Wani S, Nones K, Waddell N, et al. MicroRNA-182-5p targets a network of genes involved in DNA repair. RNA. 2013;19(2):230–42.
35. Lal A, Thomas MP, Altschuler G, Navarro F, O'Day E, Li XL, et al. Capture of microRNA-bound mRNAs identifies the tumor suppressor miR-34a as a regulator of growth factor signaling. PLoS Genet. 2011;7(11):e1002363.
36. Li J, Wan Y, Guo Q, Zou L, Zhang J, Fang Y, et al. Altered microRNA expression profile with miR-146a upregulation in CD4+ T cells from patients with rheumatoid arthritis. Arthritis Res Ther. 2010;12(3):R81.
37. Pillai MM, Gillen AE, Yamamoto TM, Kline E, Brown J, Flory K, et al. HITS-CLIP reveals key regulators of nuclear receptor signaling in breast cancer. Breast Cancer Res Treat. 2014;146(1):85–97.
38. Romay MC, Che N, Becker SN, Pouldar D, Hagopian R, Xiao X, et al. Regulation of NF-kappaB signaling by oxidized glycerophospholipid and IL-1beta induced miRs-21-3p and -27a-5p in human aortic endothelial cells. J Lipid Res. 2015;56(1):38–50.
39. Skalsky RL, Corcoran DL, Gottwein E, Frank CL, Kang D, Hafner M, et al. The viral and cellular microRNA targetome in lymphoblastoid cell lines. PLoS Pathog. 2012;8(1):e1002484.
40. Wang K, Wang X, Zou J, Zhang A, Wan Y, Pu P, et al. miR-92b controls glioma proliferation and invasion through regulating Wnt/beta-catenin signaling via Nemo-like kinase. Neuro Oncol. 2013;15(5):578–88.
41. Xue Y, Ouyang K, Huang J, Zhou Y, Ouyang H, Li H, et al. Direct conversion of fibroblasts to neurons by reprogramming PTB-regulated microRNA circuits. Cell. 2013;152(1–2):82–96.
42. Zahedi A, Bondaz L, Rajaraman M, Leslie WD, Jefford C, Young JE, et al. Risk for thyroid cancer recurrence is higher in men than in women independent of disease stage at presentation. Thyroid. 2020;30(6):871–7.
43. Genpeng L, Jianyong L, Jiaying Y, Ke J, Zhihui L, Rixiang G, et al. Independent predictors and lymph node metastasis characteristics of multifocal papillary thyroid cancer. Medicine. 2018;97(5):e9619.
44. Joseph KR, Edirimanne S, Eslick GD. Multifocality as a prognostic factor in thyroid cancer: a meta-analysis. Int J Surg. 2018;50:121–5.
45. Shin JH, Baek JH, Chung J, Ha EJ, Kim JH, Lee YH, et al. Ultrasonography diagnosis and imaging-based management of thyroid nodules: revised Korean society of thyroid radiology consensus statement and recommendations. Korean J Radiol. 2016;17(3):370–95.
46. Xue S, Wang P, Liu J, Chen G. Total thyroidectomy may be more reasonable as initial surgery in unilateral multifocal papillary thyroid microcarcinoma: a single-center experience. World J Surg Oncol. 2017;15(1):62.
47. Ha M, Son YR, Kim J, Park SM, Hong CM, Choi D, et al. TEK is a novel prognostic marker for clear cell renal cell carcinoma. Eur Rev Med Pharmacol Sci. 2019;23(4):1451–8.
48. Huang H, Bhat A, Woodnutt G, Lappe R. Targeting the ANGPT-TIE2 pathway in malignancy. Nat Rev Cancer. 2010;10(8):575–85.
49. Chen S, Yu M, Ju L, Wang G, Qian K, Xiao Y, et al. The immune-related biomarker TEK inhibits the development of clear cell renal cell carcinoma (ccRCC) by regulating AKT phosphorylation. Cancer Cell Int. 2021;21(1):119.
50. Martin V, Xu J, Pabbisetty SK, Alonso MM, Liu D, Lee OH, et al. Tie2-mediated multidrug resistance in malignant gliomas is associated with upregulation of ABC transporters. Oncogene. 2009;28(24):2358–63.
51. Lee OH, Xu J, Fueyo J, Fuller GN, Aldape KD, Alonso MM, et al. Expression of the receptor tyrosine kinase Tie2 in neoplastic glial cells is associated with integrin beta1-dependent adhesion to the extracellular matrix. Mol Cancer Res. 2006;4(12):915–26.
52. Wu ZQ, Li XY, Hu CY, Ford M, Kleer CG, Weiss SJ. Canonical Wnt signaling regulates Slug activity and links epithelial-mesenchymal transition with epigenetic breast cancer 1, early onset (BRCA1) repression. Proc Natl Acad Sci USA. 2012;109(41):16654–9.
53. Tu J, Park S, Yu W, Zhang S, Wu L, Carmon K, et al. The most common RNF43 mutant G659Vfs*41 is fully functional in inhibiting Wnt signaling and unlikely to play a role in tumorigenesis. Sci Rep. 2019;9(1):18557.
54. Greenbaum D, Colangelo C, Williams K, Gerstein M. Comparing protein abundance and mRNA expression levels on a genomic scale. Genome Biol. 2003;4(9):1–8.
55. Nie L, Wu G, Zhang W. Correlation of mRNA expression and protein abundance affected by multiple sequence features related to translational efficiency in *Desulfovibrio vulgaris*: a quantitative analysis. Genetics. 2006;174(4):2229–43.

56. Tian Q, Stepaniants SB, Mao M, Weng L, Feetham MC, Doyle MJ, et al. Integrated genomic and proteomic analyses of gene expression in mammalian cells. Mol Cell Proteom. 2004;3(10):960–9.
57. Nie L, Wu G, Zhang W. Correlation between mRNA and protein abundance in *Desulfovibrio vulgaris*: a multiple regression to identify sources of variations. Biochem Biophys Res Commun. 2006;339(2):603–10.

Publisher's Note

Springer Nature remains neutral with regard to jurisdictional claims in published maps and institutional affiliations.

Ready to submit your research? Choose BMC and benefit from:

- fast, convenient online submission
- thorough peer review by experienced researchers in your field
- rapid publication on acceptance
- support for research data, including large and complex data types
- gold Open Access which fosters wider collaboration and increased citations
- maximum visibility for your research: over 100M website views per year

At BMC, research is always in progress.

Learn more biomedcentral.com/submissions